International Journal of Heat and Mass Transfer 127 (2018) 1189–1197

Contents lists available at ScienceDirect

International Journal of Heat and Mass Transfer

journal homepage: www.elsevier.com/locate/ijhmt

Element differential method for solving transient heat conduction problems

Kai Yang, Geng-Hui Jiang, Hao-Yang Li, Zhi-bo Zhang, Xiao-Wei Gao *

State Key Laboratory of Structural Analysis for Industrial Equipment, Dalian University of Technology, Dalian 116024, China

ARTICLE INFO

Article history:
Received 10 February 2018
Received in revised form 13 July 2018
Accepted 31 July 2018

Keywords:
Element differential method
EDM
Shape functions
Isoparametric elements
Transient heat conduction

ABSTRACT

In this paper, a new numerical method, Element Differential Method (EDM), is developed for solving transient heat conduction problems with variable conductivity. The key point of this method is based on the direct differentiation of shape functions of isoparametric elements used to evaluate the geometry and physical variables. A new collocation method is proposed for establishing the system of equations, in which the governing differential equation is collocated at nodes inside elements, and the flux equilibrium equation is collocated at interface nodes between elements and outer surface nodes of the problem. Attributed to the use of the Lagrange elements that can guarantee the variation of physical variables consistent through all elemental nodes, EDM has higher stability than the traditional collocation method. The other main characteristics of EDM are that no variational principle or a control volume are required to set up the system of equations and no integrals are included to form the coefficients of the system. Based on the implicit backward differentiation scheme, an unconditionally stable and non-oscillatory time marching solution scheme is developed for solving the time-dependent system equations. Numerical examples are presented to demonstrate the accuracy and efficiency of the proposed method.

1. Introduction

Transient heat transfer analysis is of great importance in many practical engineering areas [1–3]. The solution techniques to transient heat conduction problems are mainly based on analytical and numerical methods. The analytic method is accurate, but only available for isotropic homogeneous problems with simple geometries and boundary conditions, and, therefore, has limited application. The numerical method is a very flexible and robust way to solve complex heat conduction problems. The commonly used numerical methods can be classified into four types: the finite element method (FEM) [4,5], the finite volume method (FVM) [6,7], the boundary element method (BEM) [2,8] and meshless methods [9,10]. Compared to FEM and FVM, BEM is very robust for solving the heat conduction problem, since it only needs the discretization of the problem boundary into elements, rather than the whole domain, thus reducing the dimension of the problem by one [8]. However, BEM faces a critical challenge when solving non-linear [3,11], non-homogeneous [2] and transient [12–15] problems, since usually there are domain integrals concerned in the resulting integral equations, thus making BEM lose its unique advantage of boundary only discretization. To avoid this deficiency, some methods of transforming domain integrals into equivalent boundary integrals are developed and have been frequently used. In these methods, the dual reciprocity method (DRM) developed by Brebbia [8,16] is extensively employed. However, DRM requires particular solutions to basis functions, which restricts its application to complicated problems. Recently, a new transformation method, the radial integration method (RIM), has been proposed by Gao [17,18], which not only can transform any complicated domain integrals to the boundary in a unified way without using particular solutions, but also can remove various singularities appearing in the domain integrals. For solving transient heat conduction problems, Yang and Gao [19] developed a new boundary element analysis approach based on RIM, in which RIM is used to clear up the domain integral associated with the time derivative of temperatures, and the radial integral is evaluated numerically. Then a new and simple boundary-domain integral equation is presented for solving nonlinear [20] and transient nonlinear [21] heat conduction problems with temperature-dependent conductivity of materials. By considering that the numerical evaluation of the radial integrals is very time-consuming, Yang and Gao [22–24] developed a set of new analytical expressions for evaluating radial integrals appearing in the computation of several kinds of variable coefficient problems using the radial integration boundary element

* Corresponding author.
E-mail address: xwgao@dlut.edu.cn (X.-W. Gao).

https://doi.org/10.1016/j.ijheatmasstransfer.2018.07.155
0017-9310/

method (RIBEM). Through employ of the derived analytical expressions, the computational efficiency can be increased considerably.

Recently, a new robust method, element differential method (EDM) [25,26], is proposed for solving general heat conduction problems [25], elastic mechanics and thermal stress problems [26] based on the use of isoparametric elements as used in the standard FEM [4]. A set of explicit formulations of computing the first and second order spatial derivatives are derived for 2D and 3D problems. These formulations are presented for shape functions of elements and therefore can be used to any physical variables' differentiation. Since EDM can use high order isoparametric elements to compute the spatial derivatives, the computational accuracy in heat flux is higher than the frequently used FVM method. In this paper, a new type of element differential method is developed for solving transient heat conduction problems with variable conductivity for the first time. Without the complexity of solving the transient heat conduction BEM as before, the most important characteristic of the proposed method is that the derived spatial derivatives can be directly substituted into the governing equations and the heat flux equilibrium equations to form the final system of algebraic equations. So EDM is very easy to be coded in dealing with transient heat conduction engineering problems with complicated governing equations and boundary conditions.

2. Governing equations for non-homogeneous transient heat conduction problems

The governing equation for transient heat conduction problems in isotropic non-homogeneous media can be expressed as follows:

$$\frac{\partial}{\partial x_i}\left(k_{ij}(\mathbf{x})\frac{\partial T(\mathbf{x},t)}{\partial x_j}\right)+Q(\mathbf{x})=\rho c\left(\frac{\partial T(\mathbf{x},t)}{\partial t}\right)\qquad t\geqslant t_0,\mathbf{x}\in\Omega \tag{1}$$

The boundary conditions of the problem are

$$T(\mathbf{x})=f(\mathbf{x}),\quad \mathbf{x}\in\Gamma_1\quad \text{for Dirichlet boundary condition} \tag{2a}$$

$$q_i(\mathbf{x})=-k_{ij}\frac{\partial T(\mathbf{x})}{\partial x_j}=g_i(\mathbf{x}),\ \mathbf{x}\in\Gamma_2$$
$$\text{for Neumann boundary condition} \tag{2b}$$

$$q_{\mathbf{n}}(\mathbf{x})=-k_{ij}\frac{\partial T(\mathbf{x})}{\partial x_j}n_i=h(x)(T(\mathbf{x})-T_\infty),\ \mathbf{x}\in\Gamma_3$$
$$\text{for Robin boundary condition} \tag{2c}$$

where x_i is the i th component of the spatial coordinates at point $\mathbf{x}=(x_1,x_2,\ldots,x_{ndim})$, $ndim$ the dimension of problems, $k(\mathbf{x})$ the thermal conductivity, $T(\mathbf{x})$ the temperature, and $Q(\mathbf{x})$ the heat-generation rate.

3. Derivatives of elemental shape functions with respect to global coordinates

Any variables varying over an isoparametric element can be represented in terms of their nodal values of the element [4]. For example, the spatial coordinates and temperature can be interpolated as

$$x_i=N_\alpha x_i^\alpha,\quad T=N_\alpha T^\alpha \tag{3}$$

where x_i^α, N_α and T^α are the values of coordinates, shape function and temperature at node α, respectively, and the repeated index α represents the summation over all nodes. To numerically compute the partial derivatives appearing in the governing Eq. (1) and boundary conditions (2), the analytical expressions for the first and second partial derivatives need to be derived. From Eq. (3) it follows that

$$\frac{\partial T}{\partial x_i}=\frac{\partial N_\alpha}{\partial x_i}T^\alpha,\quad \frac{\partial^2 T}{\partial x_i\partial x_j}=\frac{\partial^2 N_\alpha}{\partial x_i\partial x_j}T^\alpha \tag{4}$$

It can be seen that N_α are the explicit functions of intrinsic coordinates $\boldsymbol{\xi}=(\xi_1,\xi_2,\ldots,\xi_{ndim})$, thus

$$\frac{\partial T}{\partial x_i}=\frac{\partial N_\alpha}{\partial x_i}T^\alpha=\frac{\partial N_\alpha}{\partial \xi_j}\frac{\partial \xi_j}{\partial x_i}T^\alpha=\frac{\partial N_\alpha}{\partial \xi_j}[J]^{-1}_{ij}T^\alpha \tag{5}$$

$$\frac{\partial^2 T}{\partial x_i\partial x_k}=\frac{\partial}{\partial x_k}\frac{\partial N_\alpha}{\partial \xi_j}[J]^{-1}_{ij}T^\alpha=\left([J]^{-1}_{ij}\frac{\partial^2 N_\alpha}{\partial \xi_j\partial \xi_l}+\frac{\partial [J]^{-1}_{ij}}{\partial \xi_l}\frac{\partial N_\alpha}{\partial \xi_j}\right)[J]^{-1}_{kl}T^\alpha \tag{6}$$

where $[J]=[\partial\mathbf{x}/\partial\boldsymbol{\xi}]$ is the Jacobian matrix mapping from the global coordinate system x_i to the intrinsic coordinate system ξ_j, and $\partial\xi_l/\partial x_k$ can be determined by the following matrix relationship [4]:

$$\left[\frac{\partial\boldsymbol{\xi}}{\partial\mathbf{x}}\right]=[J]^{-1}=\left[\frac{\partial\mathbf{x}}{\partial\boldsymbol{\xi}}\right]^{-1} \tag{7}$$

where

$$\left[\frac{\partial\mathbf{x}}{\partial\boldsymbol{\xi}}\right]_{ij}=\frac{\partial x_i}{\partial\xi_j}=\frac{\partial N_\alpha}{\partial\xi_j}x_i^\alpha \tag{8}$$

The isoparametric elements used in FEM [4,5] have excellent features in geometry expression and physical variable interpolation. Referring to Ref. [25], the first and second partial derivatives needed in solving PDEs can be determined analytically by using the shape functions of isoparametric elements and a system of equations can be formed by substituting these spatial derivatives into the governing equation and boundary conditions.

4. Assembling system of equations from governing equations and boundary conditions

When solving a boundary value problem managed by a partial differential equation using EDM, the computational domain needs to be discretized into a series of isoparametric elements and nodes as done in FEM. The first and second spatial derivatives of physical variables can be calculated using Eqs. (4)-(6). Based on this, a system of equations can be directly formed by substituting Eq. (4) into the governing equation for internal nodes and boundary conditions for boundary nodes.

4.1. Setting up equations for internal nodes of elements based on the governing differential equation

For nodes located within an element, the governing equation (1) should be satisfied. To facilitate the use of EDM, Eq. (1) can be written as

$$\frac{\partial k_{ij}(\mathbf{x})}{\partial x_i}\frac{\partial T(\mathbf{x})}{\partial x_j}+k_{ij}(\mathbf{x})\frac{\partial^2 T(\mathbf{x})}{\partial x_i\partial x_j}+Q(\mathbf{x})=\rho c\left(\frac{\partial T(\mathbf{x})}{\partial t}\right) \tag{9}$$

Substituting Eq. (4) into Eq. (9) leads to

$$\left[\frac{\partial k_{ij}(\boldsymbol{\xi})}{\partial x_i}\frac{\partial N_\alpha(\boldsymbol{\xi})}{\partial x_j}+k_{ij}(\boldsymbol{\xi})\frac{\partial^2 N_\alpha(\boldsymbol{\xi})}{\partial x_i\partial x_j}\right]T^\alpha+Q(\boldsymbol{\xi})=\rho c\left(\frac{\partial T}{\partial t}\right)\quad \boldsymbol{\xi}\in\Omega \tag{10}$$

where $\boldsymbol{\xi}$ is the intrinsic coordinate at the node inside the element. The term $\partial k_{ij}/\partial x_i$ in Eq. (10) can be calculated through direct differentiation, if the analytical expression of the heat conductivity k_{ij} is given, otherwise the following expression can be used to compute its value.

$$\frac{\partial k_{ij}(\boldsymbol{\xi})}{\partial x_i}=\frac{\partial N_\beta(\boldsymbol{\xi})}{\partial x_i}k_{ij}^\beta \tag{11}$$

where k_{ij}^{β} is the value of k_{ij} at the element node β.

From Eq. (10), it follows that

$$\rho c\frac{\partial T^i}{\partial t}-\sum_{m=I_1}^{I_{nnode}}A_{im}^e T^m=Q_i,\quad i=1,2,..,N^{in} \tag{12}$$

where

$$A_{im}^e=\frac{\partial k_{ij}}{\partial x_i}\frac{\partial N_m(\xi)}{\partial x_j}+k_{ij}\frac{\partial^2 N_m(\xi)}{\partial x_i\partial x_j},\quad m\in\mathbf{I} \tag{13}$$

where $\mathbf{I}=(I_1,I_2,\ldots,I_{nnode})$ is the subscript set of the node number of an element, *nnode* is the total number of node in an element and N^{in} is the number of total nodes within all elements in the computational domain. If there are N^{in} internal nodes that aren't shared by two or more elements, there are N^{in} equations like Eq. (12).

4.2. Setting up equations for element interface nodes based on flux equilibrium conditions

For a node situated on the interface shared by a few elements, the relationship between the flux and temperature gradient, i.e. Eq. (2b), is applied to each surface including the node. In terms of the flux equilibrium condition $\sum_{f=1}^{M}q^f(\xi^I)=0$, the following equation can be establish by substituting Eq. (4) into Eq. (2):

$$\sum_{f=1}^{M}\sum_{\alpha=I_1^f}^{I_n^f}-k_{ij}\frac{\partial N_\alpha(\xi)}{\partial x_j}n_i^f T^\alpha=0,\xi^i\in\Gamma_I \tag{14}$$

where M is the number of element surfaces associated with the interface node expressed by the intrinsic coordinate ξ^i which is different for different elements, the n_i^f is the outward normal to the surface f, and Γ_I represents the interface between elements, as shown in Ref. [25].

4.3. Setting up equations for outer boundary nodes based on flux equilibrium conditions

For a node located on the outer boundary of the problem, the heat flux equilibrium condition $\sum_{f=1}^{M}q^f(\xi^b)=q(\xi^b)$ is used, where M is the number of element surfaces associated with the boundary node ξ^b, and q is the external heat flux. Thus, substituting Eq. (4) into Eq. (2), it follows that

$$\sum_{f=1}^{M}\sum_{\alpha=I_1^f}^{I_n^f}-k_{ij}\frac{\partial N_\alpha(\boldsymbol{\xi}^{\mathbf{b}})}{\partial x_j}n_i^f T^\alpha=q(\boldsymbol{\xi}^{\mathbf{b}}) \tag{15}$$

where $q(\boldsymbol{\xi}^{\mathbf{b}})=\bar{q}$, for $\boldsymbol{\xi}^{\mathbf{b}}\in\Gamma_2$; and $q(\boldsymbol{\xi}^{\mathbf{b}})=h(\boldsymbol{\xi}^{\mathbf{b}})(T(\boldsymbol{\xi}^{\mathbf{b}})-T_\infty)$, for $\boldsymbol{\xi}^{\mathbf{b}}\in\Gamma_3$.

To solve the Eq. (12), we adopt θ-method to approximate the time derivative term:

$$\left(\frac{\partial T}{\partial t}\right)_{t=t_n+\theta\Delta t}=\frac{T_{n+1}-T_n}{\Delta t} \tag{16}$$

The temperature at $t_n+\theta\Delta t$ is obtained by linear interpolation

$$T(t_n+\theta\Delta t)=(1-\theta)T_n+\theta T_{n+1} \tag{17}$$

where T^n represents the temperature at the n-th time step, and θ is the Euler parameter which usually takes a value between 0.5 and 1. If $\theta=0$, the explicit Euler method is adopted, θ=0.5 the Crank-Nicolson method, and $\theta=1$ the implicit Euler method. According to Ref. [27], the Crank-Nicolson method can become restrictly stable if the boundary conditions are not correctly set, but it is an unconditionally stable second-order accurate method. And the implicit Euler method is always unconditionally stable.

Let

$$R_i=\sum_{m=I_1}^{I_n}A_{im}^e T^m+Q_i,i=1,2,..,N \tag{18}$$

Substituting Eqs. (16) and (17) into Eq. (12), and considering Eq. (18), it follows that

$$\rho c\frac{T_{n+1}-T_n}{\Delta t}-[(1-\theta)R_n+\theta R_{n+1}]=0 \tag{19}$$

The temperature at t_{n+1}, satisfies the relation

$$\sum_{m=I_1}^{I_n}\bar{A}_{im}^e T_{n+1}^m=\bar{Q}_i,i=1,2,..,N \tag{20}$$

where

$$\bar{A}_{im}^e=\frac{\rho c}{\Delta t}-A_{im}^e \tag{21}$$

$$\bar{Q}_i=Q_i+\rho c\frac{T_n^i}{\Delta t}-\sum_{m=I_1}^{I_n}A_{im}^e T_n^m \tag{22}$$

Substituting Eqs. (16) and (17) into Eqs. (14) and (15) lead to

$$\sum_{f=1}^{M}\sum_{\alpha=I_1^f}^{I_n^f}-\theta k_{ij}\frac{\partial N_\alpha(\xi)}{\partial x_j}n_i^f T_{n+1}^\alpha=\sum_{f=1}^{M}\sum_{\alpha=I_1^f}^{I_n^f}(1-\theta)k_{ij}\frac{\partial N_\alpha(\xi)}{\partial x_j}n_i^f T_n^\alpha \tag{23}$$

$$\sum_{f=1}^{M}\sum_{\alpha=I_1^f}^{I_n^f}-\theta k_{ij}\frac{\partial N_\alpha(\boldsymbol{\xi}^{\mathbf{b}})}{\partial x_j}n_i^f T_{n+1}^\alpha=q(\boldsymbol{\xi}^{\mathbf{b}})+\sum_{f=1}^{M}\sum_{\alpha=I_1^f}^{I_n^f}(1-\theta)k_{ij}\frac{\partial N_\alpha(\boldsymbol{\xi}^{\mathbf{b}})}{\partial x_j}n_i^f T_n^\alpha \tag{24}$$

Note that Eqs. (23) and (24) are the conservation of heat flux, independent of time. When $\theta=0$, the left side of the equation is equal to 0 and the right side contains only the temperature values that have been derived at the previous moment. Therefore $0<\theta\leqslant 1$.

4.4. Forming the final system of equations

Applying ξ in Eq. (20) to all internal nodes, $\boldsymbol{\xi}^{\mathbf{I}}$ in Eq. (23) to all interface nodes, $\boldsymbol{\xi}^{\mathbf{b}}$ in Eq. (24) to all outer boundary nodes of all elements, each of them can generate an equation including nodal temperatures and heat fluxes. For interface nodes shared by a few elements, the temperature continuous condition, $T^I=T^{II}$, is used, where T^I and T^{II} are the temperatures over the adjacent elements I and II, respectively, and they have the same position in the global temperature vector. For each outer boundary node, either the temperature or the heat flux is specified. Thus, multiplying the specified temperatures and fluxes in Eqs. (20)–(24) with corresponding coefficients to form a known vector $\mathbf{b}$ and moving it to the right-hand side of the system of equations, and the remaining terms associated with unknown temperatures and unknown fluxes being put on the left-hand side of the system of equations, the final system of equations can be formed as

$$\mathbf{Ax}=\mathbf{b} \tag{25}$$

where $\mathbf{x}$ is a vector including each nodal unknown temperature or unknown flux. By solving Eq. (25) for vector $\boldsymbol{x}$, we can get all unknowns of the problem. It is noted that if the total number of all nodes is N, then the dimension of the coefficient matrix $\mathbf{A}$ in Eq. (25) is $N\times N$.

5. Numerical examples

A computer code called EDM has been developed using the formulations derived in this paper. To verify the correctness of the derived formulations, three numerical examples are presented in the following.

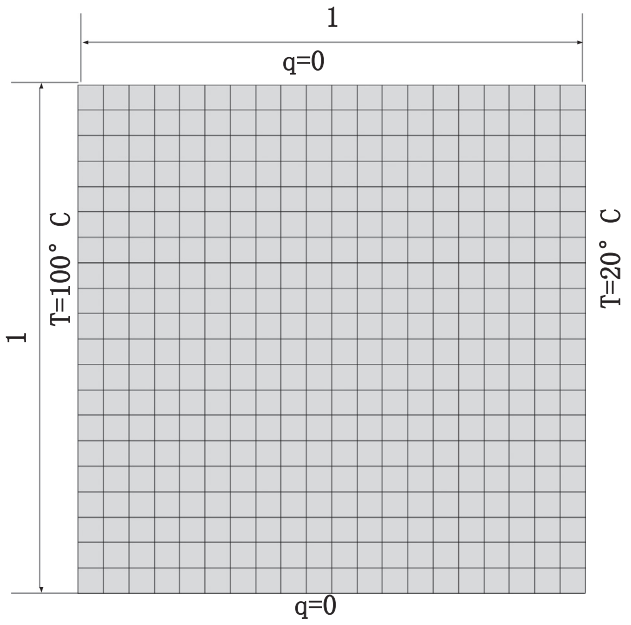

Fig. 1. Boundary conditions and mesh of the 2D square.

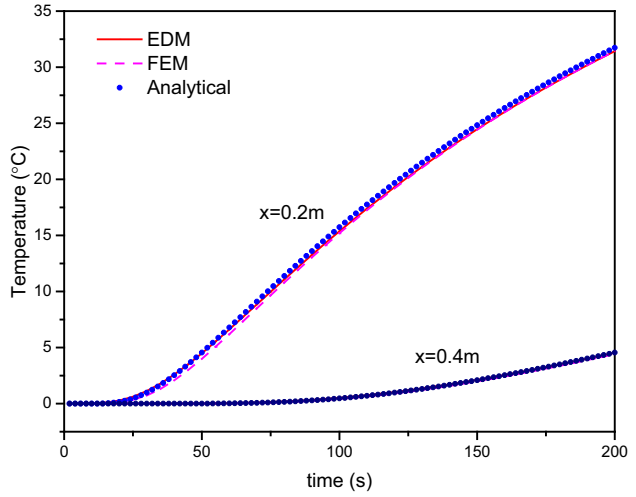

Fig. 2. Computed temperature for the plate versus time.

Table 1
The error compared with EDM and FEM at $x = 0.2$ m.

t	EDM	FEM	Analytical	EDM error	FEM error
40	2.59369	2.07956	2.53636	0.00057	−0.00457
60	6.62385	6.19582	6.79133	−0.00167	−0.00596
80	11.08520	10.80430	11.38762	−0.00302	−0.00583
100	15.37512	15.20040	15.73335	−0.00358	−0.00533
120	19.30309	19.19690	19.67433	−0.00371	−0.00477
140	22.84015	22.77770	23.20383	−0.00364	−0.00426
160	26.01255	25.97840	26.35954	−0.00347	−0.00381
180	28.86170	28.84610	29.18855	−0.00327	−0.00342
200	31.42968	31.42640	31.73571	−0.00306	−0.00309

5.1. Heat conduction over a unit square plate

The first example considered is a plate of 1 m × 1 m with thermal conductivity $k = 100$ W/(m·° C). The initial temperature is 0 °C. The density is $\rho = 5000$ kg/m^3, the specific heat is $C = 200$ J/(kg·° C). The top and bottom boundaries are insulated, while the left and right walls are imposed with temperatures of 100 °C and 0 °C, as shown in Fig. 1. Performing Laplace transform on time for Eq. (1) and substituting it into boundary conditions, it follows that

$$\bar{T}(x) = 100\frac{e^{(x-2)\sqrt{s\rho c/k}} - e^{-x\sqrt{s\rho c/k}}}{s(e^{-2\sqrt{s\rho c/k}} - 1)}, \bar{T} = \int_0^{+\infty} Te^{-st}dt \tag{26}$$

Then, the expressions are inverted back into the time domain. But, these expressions are too complicated for direct inverting. So, we use the Riemann-sum approximation method:

$$T(x,t) = \frac{e^{\beta t}}{t}\left(\frac{1}{2}\overline{T}(x,\beta) + Re\sum_{i=1}^{n}\overline{T}(x,\beta + \frac{in\pi}{t})(-1)^n\right) \tag{27}$$

where Re means the real part and i is the imaginary number unit. For faster convergence, numerous numerical experiments [28] have shown that the value of β satisfies the relation of $\beta t \approx 4.7$.

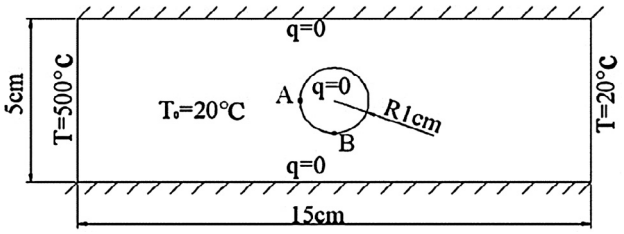

Fig. 3. Dimensions and boundary conditions of the plate.

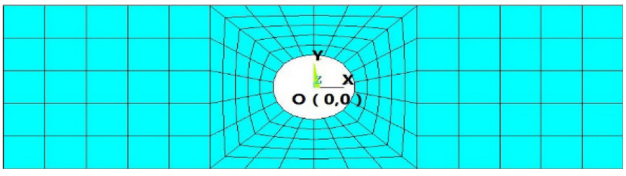

Fig. 4. EDM mesh of 9-node Lagrange elements.

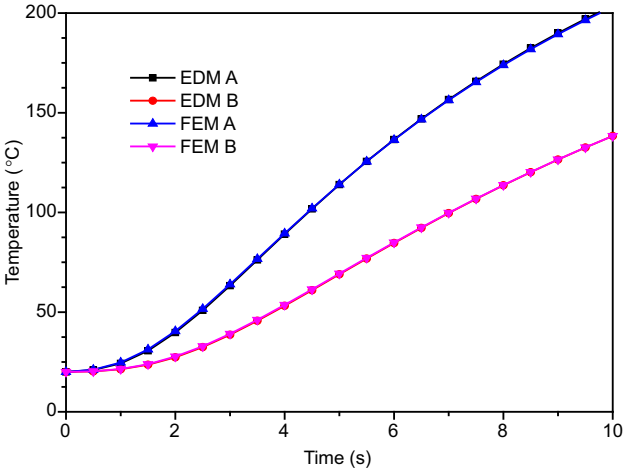

Fig. 5. Distribution of temperature versus time at point A and B.

To use the formulations presented in this paper, the plate is discretized into 100 equally-spaced 9-node 2D rectangular elements with 441 nodes as shown in Fig. 1. The temperatures at 20 internal points are investigated, which are located at x = 0.2 m and x = 0.4 m. The whole computation time is 200 s, which is divided into 40 time steps with Δt =5s for each time step. For comparison, analytical

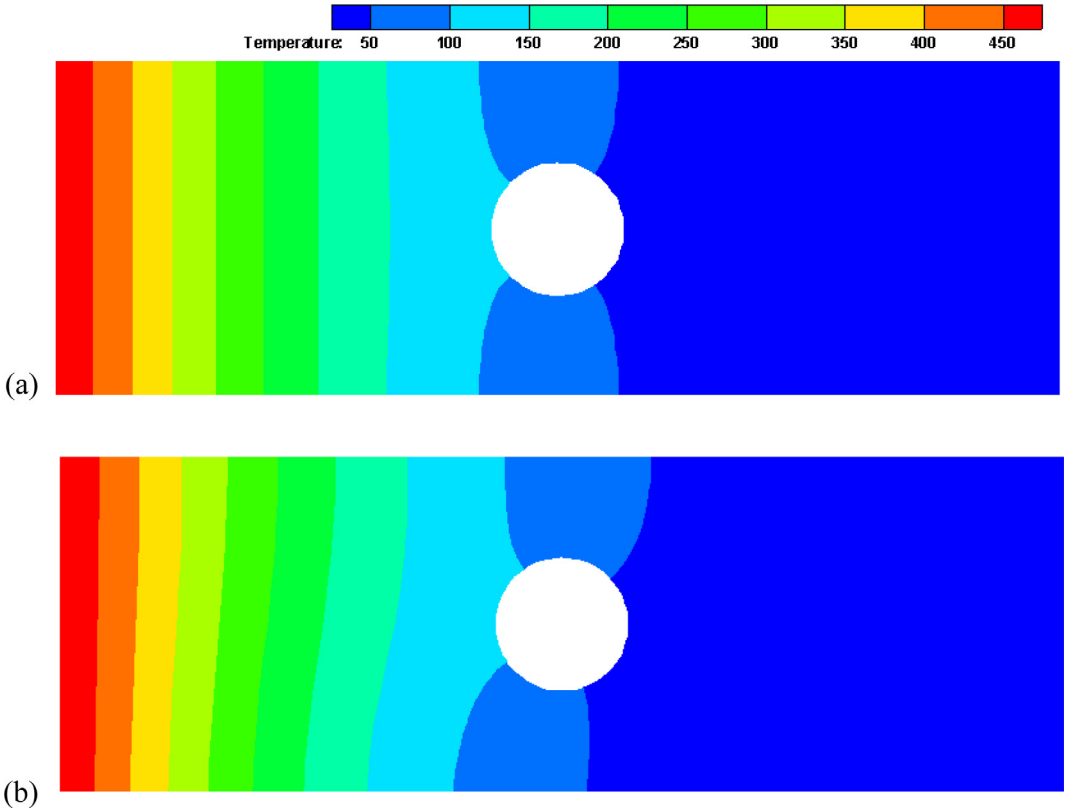

Fig. 6. Temperature contour at t = 5 s, (a) constant conductivity, (b) varying conductivity.

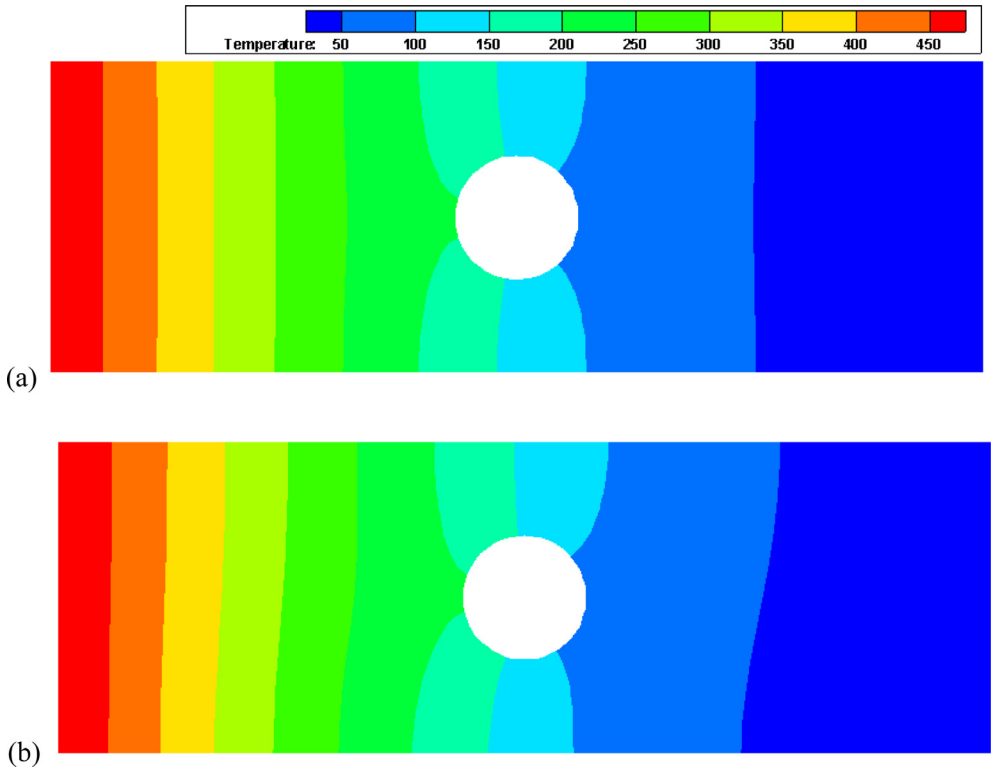

Fig. 7. Temperature contour at t = 10 s, (a) constant conductivity, (b) varying conductivity.

solutions and the FEM software ANSYS results are also provided. Fig. 2 shows the computed results using EDM along the line of x = 0.2 m and x = 0.4 m using different time steps, respectively. From Fig. 2, it can be seen that the computational results are in good agreement with the analytical solutions and FEM results. This indicates that the proposed method is correct. The error in Table 1 is define as

$$error = \frac{T_{numerical} - T_{exact}}{T_{ref}}, T_{ref} = 100 \tag{28}$$

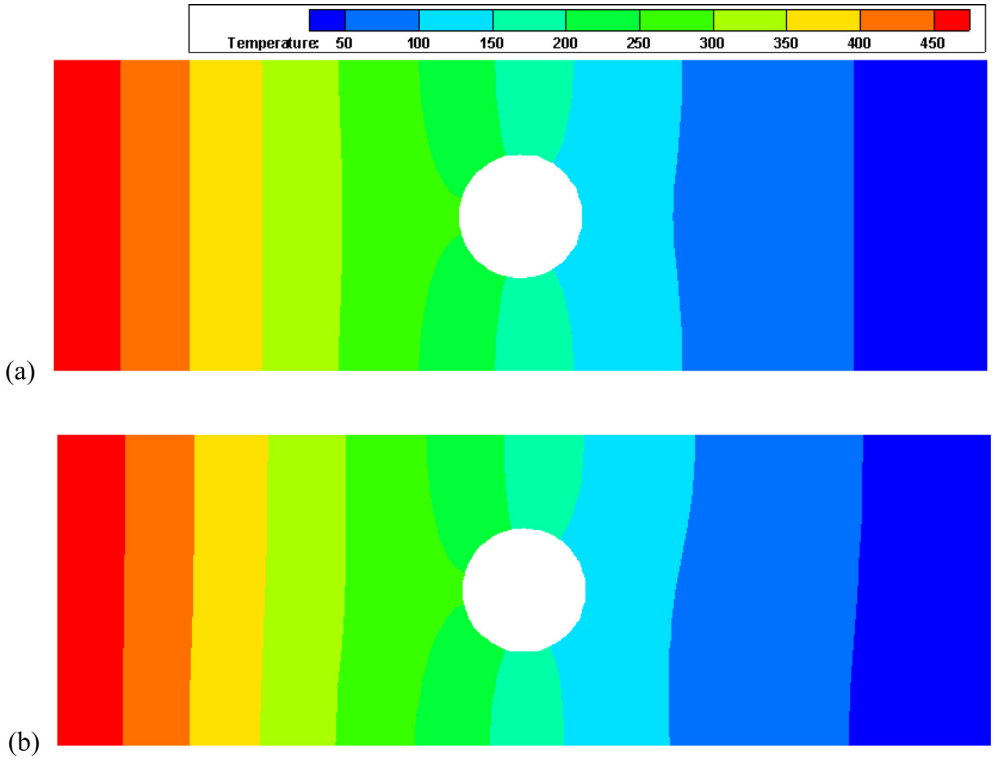

Fig. 8. Temperature contour at t = 15 s, (a) constant conductivity, (b) varying conductivity.

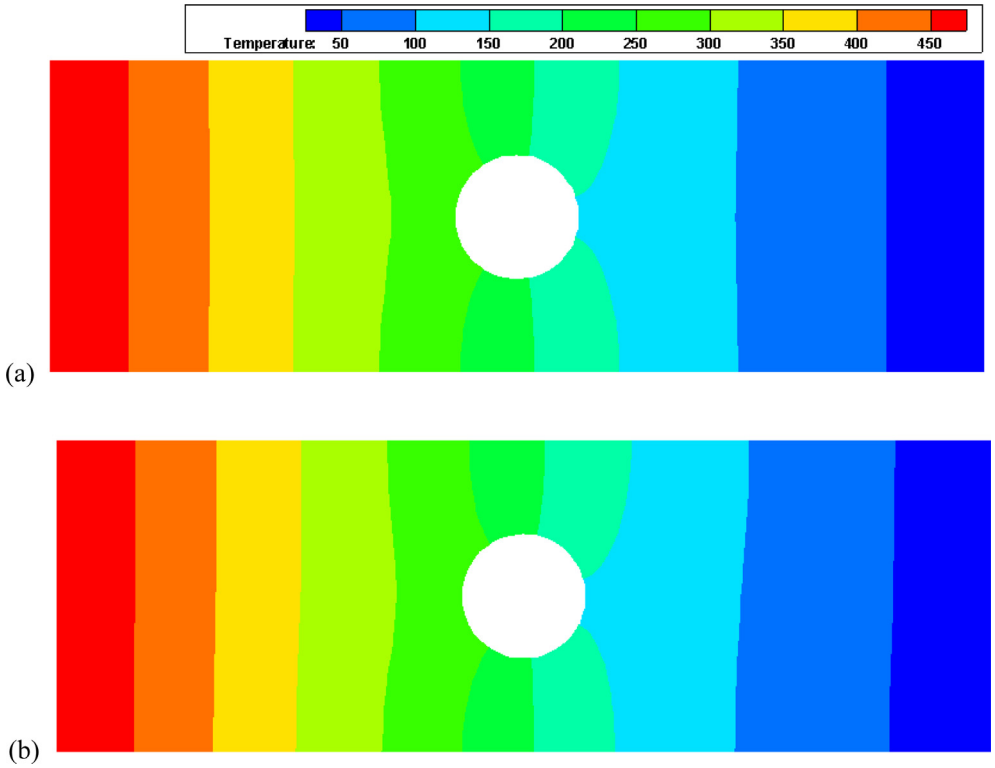

Fig. 9. Temperature contour at t = 20 s, (a) constant conductivity, (b) varying conductivity.

From Table 1, it can be seen that the presented EDM results are a little bit more accurate than FEM results.

5.2. Heat conduction over a plate with a circular perforation

In the second example, a rectangular plate with a hole is analyzed. The geometry and boundary conditions are shown in Fig. 3. The top and bottom sides as well as the boundary of the hole are insulated. The specific heat $C = 200\,\mathrm{J/(kg\cdot^\circ C)}$ and density $\rho = 5000\,\mathrm{kg/m^3}$. Two cases are computed, one for constant heat conductivity of $k = 200\,\mathrm{W/(m\cdot^\circ C)}$, and the other for varying thermal conductivity along the y-direction of $k = 200 + 4000\mathrm{y}\ \mathrm{W/(m\cdot^\circ C)}$ .The plate is discretized into 160 9-node Lagrange elements and 704 nodes, as shown in Fig. 4. The initial temperature is $T_0 = 20\,^\circ\mathrm{C}$, the temperature on the left boundary of the plate is suddenly increased to $T = 500\,^\circ\mathrm{C}$, while the right boundary keeps a constant temperature of 20 °C. The temperatures at point A and B are investigated as marked in Fig. 3. Fig. 4 shows the EDM model for computation.

The time marching process is divided into 50 time steps. The length of each time steps is $\Delta t = 0.5$ s. For comparison, the problem is also computed using the FEM software ANSYS. Fig. 5 gives the comparison of the computed temperatures between FEM and the presented EDM at various time for point A and B, and Figs. 6–9 are the contour plots of the computed temperature using time steps of 5, 10, 15, and 20 s, respectively.

From Fig. 5, it can be seen that the presented EDM results are in excellent agreement with FEM results. Figs. 6–9 show that the results computed using constant and varying conductivities are obviously different at the beginning of the time period, but gradually become identical when stability is achieved.

5.3. Convection heat transfer over a 3D radiator

The third example is the convection heat transfer analysis of a 3D radiator. The geometry and boundary conditions of the radiator are shown in Fig. 10. The heat conductivity $k = 100\,\mathrm{W/(m\cdot^\circ C)}$, specific heat $C = 200\,\mathrm{J/(kg\cdot^\circ C)}$, convection heat transfer coefficient $h = 100\,\mathrm{W/(m^2\cdot^\circ C)}$ and density $\rho = 5000\,\mathrm{kg/m^3}$. The environment temperature is $T_\infty = 20\,^\circ\mathrm{C}$, and the initial temperature is $T_0 = 20\,^\circ\mathrm{C}$, the temperature on the bottom boundary of the radiator is suddenly increased to $T_b = 100\,^\circ\mathrm{C}$, while other surfaces remain unchanged. The radiator is discretized into 4400 27-node Lagrange elements and 40,631 nodes, as shown in Fig. 11. The temperatures at point A and B are investigated.

The time marching process is divided into 100 time steps. The length of each time step is $\Delta t = 1$ s. For comparison, the problem is also computed using the FEM software ANSYS. EDM program stores the sparse matrix into hard disk to save computer memory, and the total computational time spended on this problem is 2103 s on 3.4G Core I5 670 CPU. Each time step costs 18 s to form the equations and 3 s to solve the system. While Commercial software Ansys cost 797 s on this problem. Fig. 12 shows the comparison of the computed temperatures between FEM and the presented EDM at various time for point A and B as marked in Fig. 11, and Fig. 13 is the temperature distribution along the line CD at t = 100 s. Fig. 14 shows the contour plot of the computed temperature using EDM with time steps of 25, 50, 75, and 100 s, respectively.

From Figs. 12 and 13, it can be seen that the presented EDM results are in excellent agreement with FEM results and from Fig. 14, it can be clearly seen that the entire convection heat transfer process changes with time.

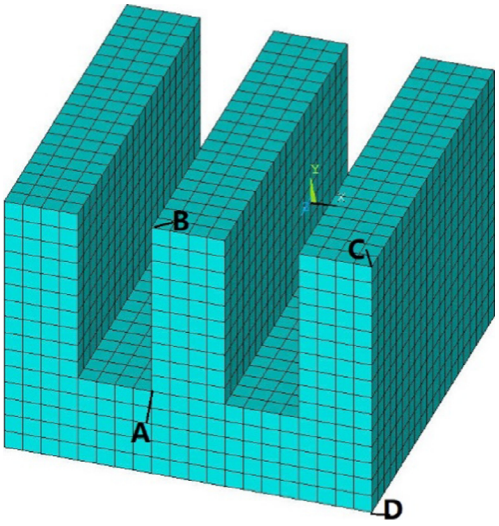

Fig. 11. Computational mesh used in EDM.

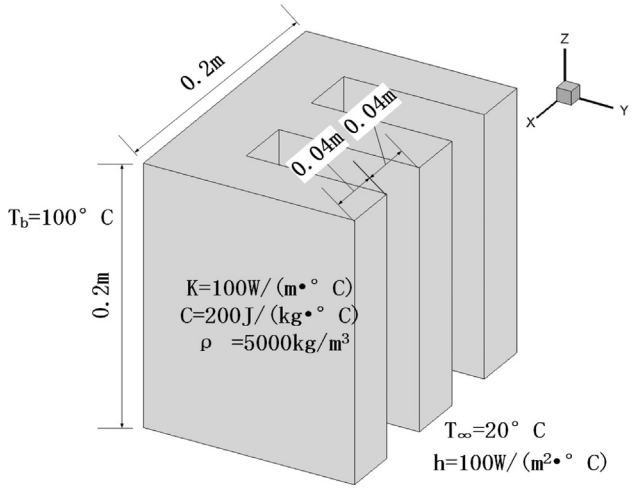

Fig. 10. Dimensions and boundary conditions of the radiator.

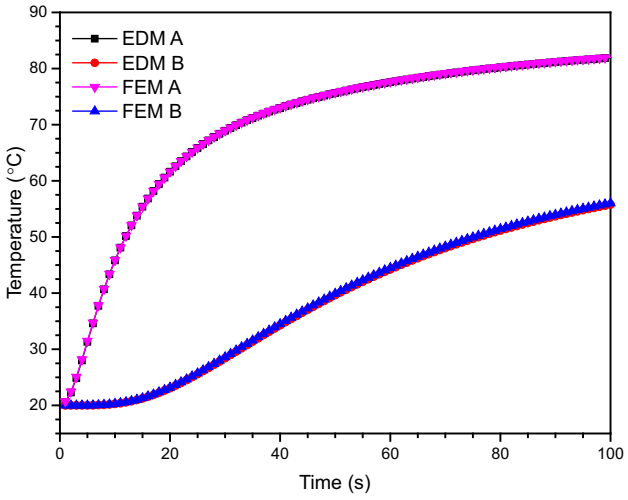

Fig. 12. Distribution of temperature versus time at point A and B.

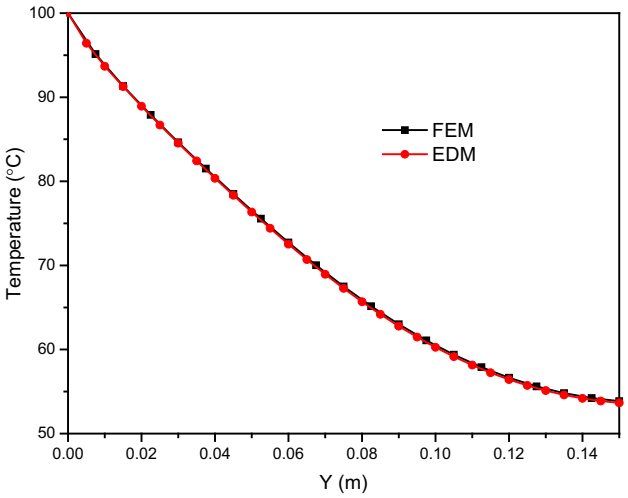

Fig. 13. Distribution of temperature alone the line CD at t = 100 s.

6. Conclusions

In this paper, a new and robust method, element differential method (EDM) has been proposed for solving transient heat conduction problems with variable thermal conductivity. EDM is a strong-form technique, which borrows the idea of FEM in the aspect of using isoparametric elements to get the spatial derivatives, and the idea of collocation-like mesh free method (MFM) in the aspect of collocating equations at nodes. Thus, it is easier to be coded than FEM, more accurate and more stable results than the traditional collocation method. Based on the central finite difference technique, an implicit time marching solution scheme is developed for solving the time-dependent system of equations. The given numerical examples have demonstrated the correctness of the developed method.

Acknowledgements

The author gratefully acknowledges the National Natural Science Foundation of China for financial support to this work under Grant NSFC Nos. 11572075 and 11672061.

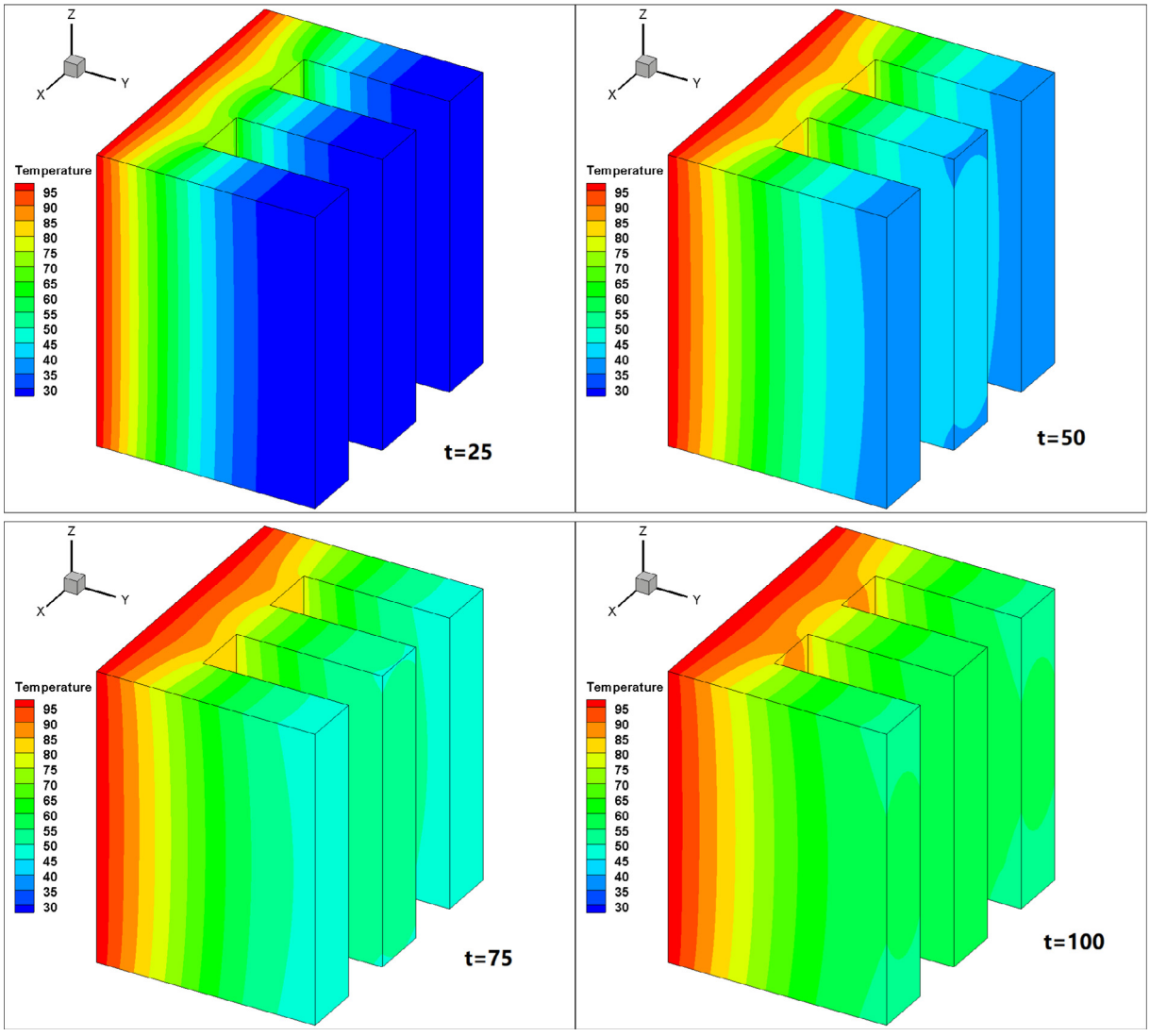

Fig. 14. Temperature contour at t = 25 s, 50 s, 75 s, 100 s.

Conflict of Interest

The authors declare that they have no conflict of interest.

References

[1] E.A. Divo, A.J. Kassab, Boundary element methods for heat conduction: with applications in non-homogeneous media, WIT Press, Southampton, 2003.
[2] J. Sladek, V. Sladek, S.N. Atluri, Local boundary integral equation (LBIE) method for solving problems of elasticity with nonhomogeneous material properties, Comput. Mech. 24 (2000) 456–462.
[3] S.Z. Feng, X.Y. Cui, A.M. Li, Fast and efficient analysis of transient nonlinear heat conduction problems using combined approximations method, Int. J. Heat Mass Tran. 97 (2016) 638–644.
[4] O.C. Zienkiewicz, R.L. Taylor, The Finite Element Method, McGraw-Hill, London, 1989.
[5] G.R. Liu, S.S. Quek, The Finite Element Method: A Practical Course, Second ed., Butterworth-Heinemann, Oxford, 2013.
[6] W.Q. Tao, Y.L. He, Q.W. Wang, Z.G. Qu, F.Q. Song, A unified analysis on enhancing single phase convective heat transfer with field synergy principle, Int. J. Heat Mass Tran. 45 (2002) 4871–4879.
[7] Y.B. Tao, Y.L. He, Y.K. Liu, W.Q. Tao, Performance optimization of two-stage latent heat storage unit based on entransy theory, Int. J. Heat Mass Tran. 77 (2014) 695–703.
[8] C.A. Brebbia, J.C. Telles, L.C. Wrobel, Boundary Element Techniques, Springer, Berlin, 1984.
[9] M. Dehghan, R. Salehi, A meshfree weak-strong (MWS) form method for the unsteady magnetohydrodynamic (MHD) flow in pipe with arbitrary wall conductivity, Comput. Mech. 52 (2013) 1445–1462.
[10] M. Dehghan, M. Abbaszadeh, Proper orthogonasl decomposition variational multiscale element free galerkin (POD-VMEFG) meshless method for solving incompressible Navier-Stokes equation, Comput. Methods Appl. Mech. Engrg. 311 (2016) 856–888.
[11] A. Khosravifard, M.R. Hematiyan, L. Marin, Nonlinear transient heat conduction analysis of functionally graded materials in the presence of heat sources using an improved meshless radial point interpolation method, Appl. Math. Model. 35 (2011) 4157–4174.
[12] E. Divo, A.J. Kassab, Boundary Element Method for Heat Conduction: With Applications in Non-Homogenous Media, WIT press, Southampton, 2003.
[13] V. Sladeka, J. Sladeka, M. Tanakab, C. Zhang, Transient heat conduction in anisotropic and functionally graded media by local integral equations, Eng. Anal. Bound. Elem. 29 (2005) 1047–1065.
[14] M. Dehghan, M. Safarpoor, The dual reciprocity boundary elements method for the linear and nonlinear two-dimensional time-fractional partial differential equations, Math. Meth. Appl. Sci. 39 (2016) 3979–3995.
[15] D. Mirzaei, M. Dehghan, New implementation of MLBIE method for heat conduction analysis in functionally graded materials, Eng. Anal. Bound. Elem. 36 (2012) 511–519.
[16] P.W. Partridge, C.A. Brebbia, L.C. Wrobel, The dual reciprocity boundary element method, Computational Mechanics Publications, Southampton, 1992.
[17] X.W. Gao, The radial integration method for evaluation of domain integrals with boundary-only discretization, Eng. Anal. Bound. Elem. 26 (2002) 905–916.
[18] X.W. Gao, A meshless BEM for isotropic heat conduction problems with heat generation and spatially varying conductivity, Int. J. Numer. Meth. Eng. 66 (2006) 1411–1431.
[19] K. Yang, X.W. Gao, Radial integration BEM for transient heat conduction problems, Eng. Anal. Bound. Elem. 34 (2010) 557–563.
[20] K. Yang, J. Wang, J.M. Du, H.F. Peng, X.W. Gao, Radial integration boundary element method for nonlinear heat conduction problems with temperature-dependent conductivity, Int. J. Heat Mass Tran. 104 (2017) 1145–1151.
[21] K. Yang, H.F. Peng, J. Wang, C.H. Xing, X.W. Gao, Radial integration BEM for solving transient nonlinear heat conduction with temperature-dependent conductivity, Int. J. Heat Mass Tran. 108 (2017) 1551–1559.
[22] K. Yang, W.Z. Feng, J. Li, X.W. Gao, New analytical expressions in radial integration BEM for stress computation with several kinds of variable coefficients, Comput. Methods Appl. Mech. Engrg. 289 (2015) 44–59.
[23] K. Yang, H.F. Peng, M. Cui, X.W. Gao, New analytical expressions in radial integration BEM for solving heat conduction problems with variable coefficients, Eng. Anal. Bound. Elem. 50 (2015) 224–230.
[24] K. Yang, W.Z. Feng, H.F. Peng, J. Lv, A new analytical approach of functionally graded material structures for thermal stress BEM analysis, Int. Commu. Heat Mass 62 (2015) 26–32.
[25] X.W. Gao, S.Z. Huang, M. Cui, B. Ruan, Q.H. Zhu, K. Yang, J. Lv, H.F. Peng, Element differential method for solving general heat conduction problems, Int. J. Heat Mass Tran. 115 (2017) 882–894.
[26] X.W. Gao, Z.Y. Li, K. Yang, J. Lv, H.F. Peng, M. Cui, B. Ruan, Q.H. Zhu, Element differential method and its application in thermal-mechanical problrms, Int. J. Numer. Meth. Eng (2017) 1–27.
[27] C.M. Oishi, J.Y. Yuan, J.A. Cuminato, Stability analysis of Crank-Nicolson and Euler schemes for time-dependent diffusion equations, Bit. Numer. Math. 55 (2015) 487.
[28] D.Y. Tzou, Macro-to-microscale heat transfer. Taylor & Francis, Washington, DC.